Chapter 36

Electron LINAC Based Photoneutron Source

– *Rishi Verma & Archana Sharma*

36.1 Introduction

LINAC is one of the most efficient techniques of accelerating charged subatomic particles (electrons and ions) to very high energies (up to 100's of MeV) by injecting RF in series resonant cavities along a linear beamline under high vacuum [169]. In LINAC's neutrons in wide spectrum of energies are produced by impinging highly accelerated electron beam on a suitable high-Z target [166]. This produces high energy X-rays/ photons by the Bremsstrahlung interaction where spectrum has end-point maximum energy equivalent to incident electron beam. These high energy photons then further interact with suitable photoneutron target and secondary neutrons may get produced via photonuclear (γ,n) and electro-nuclear (e,n) reactions by incident photons and electrons, respectively. In electro-nuclear (e,n) reactions, very high energy electron beams ($>$ 100 MeV) can directly interact with nucleus and produce neutron but probability/cross-section is 100× smaller than photonuclear (γ,n) reaction [170]. Since majority of LINAC systems used in wide range of applications operate up to 30 MeV hence neutron production is dominated via photonuclear (γ,n) reaction. Followed sections in this chapter provides further details on important aspects of such systems like mechanisms of photoneutron production, selection of suitable photoneutron target, typical energy of generated photoneutron, photoneutron yield and measuring of neutron flux etc.

36.2 Photoneutron Production Mechanism

The most important aspect of neutron that makes it more unique than other forms of radiation is that it has no charge and thus it is completely unaffected by electromagnetic interactions (encountered by ions and electrons) and primarily interacts with atomic nuclei rather than surrounding electron clouds. This feature makes neutrons an ideal probing tool to investigate nuclear structure of any matter. In free-state, it undergoes beta decay producing proton, electron and anti-neutrino within life time of 886 seconds [171].

$$n^0 \rightarrow p^+ + e^- + \bar{\nu}_e \tag{36.1}$$

Photonuclear reaction happens only if the energy spectrum of generated Bremsstrahlung photon is higher than the photodisintegration energy threshold of used target material. As shown in Fig. 36.1 [172], photonuclear (γ,n) reaction is mainly dominated by the indent photon energy 'k' and the processes of neutron production are categorized as Giant Dipole Resonance (GDR), Quasi-Deuterons (QD) and Photopion [172, 173].

36.2.1 Giant Dipole Resosnance (GDR)

In GDR mechanism, energy is transferred to the nucleus by high energy photon that produces giant resonance oscillation and neurons get released during de-excitation. The cross section for neutron production via GDR mechanism has maximum for photons energy between 13-18 MeV for medium and heavy nuclei and 20-23 MeV for light nuclei (A $<$ 40) and it reduces rapidly at photon energies $>$ 35 MeV. The GDR neutron yield mainly depends upon track length of photon (l) and the cross section for photoneutron by GDR as shown in Eq. (36.2) [166].

$$Y_{GDR} = \frac{6.023 \times 10^{-4} \sigma f N_n}{A E_0} \int_{E_{th}}^{E_{max}} \sigma_{GDR}(k) \left(\frac{dl}{dk} \right) dk \tag{36.2}$$

where Y$_{GDR}$ = Neutron yield by GDR (neutron-MeV^{-1}/electron), ρ = target density (g-cm^{-3}), f = natural abundance of isotope, N$_n$ = neutrons generated per photonuclear reaction, A = weight of atom (g mol^{-1}), E$_0$ = energy of electron (MeV), σ_{GDR}(k) = cross-section for

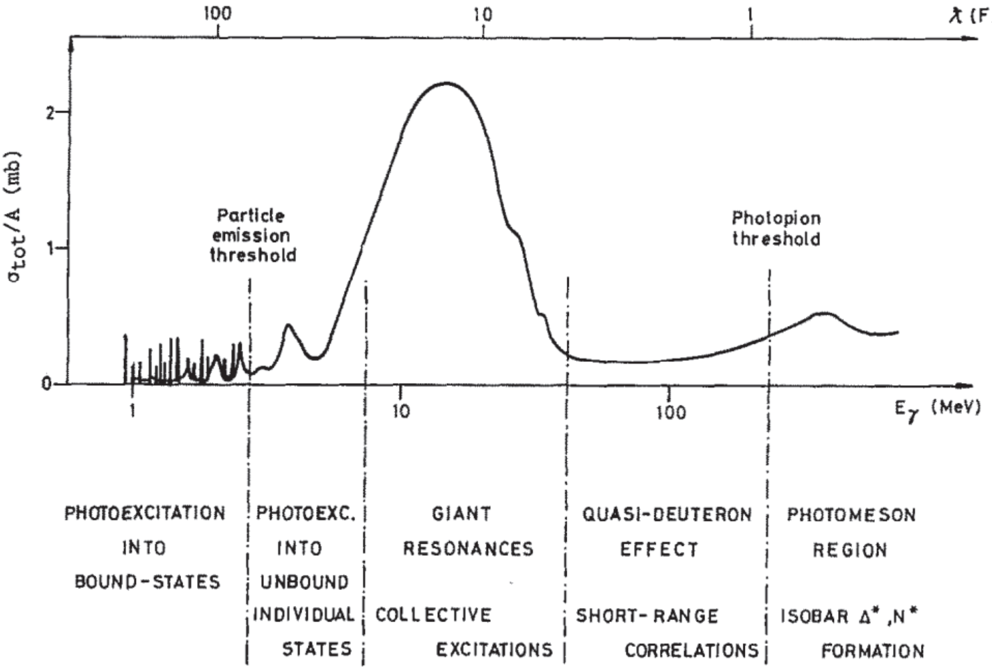

Figure 36.1: Photonuclear cross-section Vs mechanisms depending on photon energy [172].

photonuclear reaction (mb), dl/dk = varying track length of photon (cm MeV^{-1}), k = energy of photon (MeV), E_{th} = neutron separation energy threshold (MeV), E_{max} = maximum energy for photonuclear reaction (MeV).

36.2.2 Quasi-Deuteron Effect (QD)

Quasi-deuteron effect dominates when the typical energy of photons is in the range of 50 MeV to 140 MeV. In this effect interaction happens between energetic photon and neutron pair instead of nucleus, thus named ‘quasi-deuteron’. The cross-section for this mechanism is about 10× lower than the GDR [166].

36.2.3 Photopion Production

As it can be seen in Fig. 36.1, the photonuclear cross section rises again for photon energies exceeding 140 MeV and it is dominated by photopion production. Its cross-section has several resonance peaks those lying $\leq$ 1.1 GeV caused by nuclear isobar formation [166]. Neutrons generated from photopion are of much higher energy as compared to other mechanisms.

36.3 Selection of Photoneutron Targets

For the production of maximum neutron flux via photonuclear reaction appropriate choice of photoneutron target/converter material of optimum thickness has significant importance. The very first step for selection of photoneutron target is the choice of suitable material whose photodisintegration energy threshold/ neutron separation energy is lower than the incident energy of photons impinged on it [174]. Larger photonuclear cross-section of target material for the incident photon energy results in optimum neutron yield. Photoneutron targets of low-Z or high-Z materials can be used depending upon incident energy of photons and photodisintegration threshold of chosen material.

36.3.1 Targets of Low Photodisintegration Energy Threshold

Targets of low photodisintegration energy threshold are typically low-Z elements for e.g. Beryllium and Deuterium, threshold energy is 1.666 MeV and 2.226 MeV respectively. These targets are suitable for generating neutrons even from photon energies > 1.7 MeV but unfortunately the conversion efficiency of electrons to photons via Bremsstrahlung process in these low-Z targets is very small and hence double layer converter scheme is adopted to maximize photoneutron production. The first layer of converter is high-Z material (e.g. Pb, W, Ta etc) for e-γ reaction and then in the second layer suitable target of low photodisintegration energy threshold is used for the production of neutrons by γ-n reaction. Commonly used targets of low photodisintegration energy thresholds are listed in Table 36.1 [174].

Table 36.1: Nuclides having low threshold for photonuclear reaction.

Nuclide	**Threshold (MeV)**	**Reaction**
^{2}D	2.225	^{2}H(γ,n)^{1}H
^{6}Li	3.697	^{6}Li(γ, n+p)^{4}He
^{6}Li	5.67	^{6}Li(γ,n)^{5}Li
^{7}Li	7.251	^{7}Li(γ,n)^{6}Li
^{9}Be	1.667	^{9}Be(γ,n)^{8}Be

36.3.2 Targets of High Photodisintegration Energy Threshold

High-Z materials like Pb, Ta, W are most suitable single layer photoneutron targets for electron beam energies in the range of 15 MeV to 30 MeV. Neutron separation energy for these materials are typically in the range of 6 MeV to 9 MeV. Target materials having high energy threshold for photonuclear reaction are listed in Table 36.2 [175].

Table 36.2: Nuclides having high threshold for photonuclear reaction.

Nuclide	**Threshold (MeV)**
^{208}Pb, ^{207}Pb, ^{206}Pb	7.37, 6.74, 8.09
^{186}W, ^{184}W, ^{183}W, ^{182}W	7.19, 7.41, 6.19, 8.07
^{181}Ta	7.58
^{63}Cu, ^{65}Cu	10.85, 9.91
^{56}Fe	11.2
^{27}Al	13.06
^{16}O	15.66
^{12}C	18.72

36.4 Energy of Photoneutron

Photoneutron production happens only when incident photon has higher energy than separation energy required to knockout most loosely bounded neutron in the target material atom.

The typical energy of ejected neutron is approximated as [176]:

$$E_{pn} \approx \frac{(A-1)}{A}\left(E_\gamma - Q - \frac{E_\gamma^2}{2m_nc^2(A-1)} + \frac{E_\gamma}{A}\sqrt{\frac{2(A-1}{(m_nc^2A)(E_\gamma - Q)}}\cos\theta\right) \tag{36.3}$$

Where A is target mass number, E_γ is energy of incident photon, E_{pn} is generated photoneutron energy, Q is energy threshold for reaction, m_n is mass of neutron, c is speed of light, and θ is photoneutron emission angle with respect to incident beam. It may be noted that the actual energy of generated photoneutron is much less than aforementioned estimate due to intrinsic collisions. It is remarkable to note that the photoneutrons have distributed energy spectrum and the highest photoneutron energy is equivalent to the difference between maximum energy of incident photon and the threshold energy required for photonuclear reaction. Fluence averaged most probable energy of generated photoneutrons typically lies in the range of 100keV to 1 MeV e.g. refer the data shown in Table 36.3 for electron beam having energy of 9, 10, 15, 18 and 20 MeV falling on 4 mm thick Tungsten target [177]. It worth's noting that mean energy of generated Bremsstrahlung spectrum is typically about 20% of the kinetic energy of incoming electrons.

Table 36.3: Secondary particle average energies for 4mm thick target of Tungsten [177].

Energy of electron beam (MeV)	9	10	15	18	20
Average energy of photon (MeV)	2.07	2.25	2.98	3.48	3.72
Average energy of photoneutron (MeV)	0.401	0.445	0.713	0.776	0.798

36.5 Photoneutron Yield

Photoneutron yield from electron beam depends upon target material properties and its thickness, incident electron energy and fluence rate and photonuclear cross-section. The photoneutron yield from specific material is given as [173]:

$$NeutronYield, \phi_n = N_0\rho t.\sigma_T(E).\frac{\phi_e}{M}(n/s) \tag{36.4}$$

where N_0 is the Avogadro's number, M is mass of atom, ρ is density, t is target thickness, ϕ_e is incoming electron flux (electron/s), $\sigma_T(E)$ is the cumulative photonuclear cross-section for electron energy E. An overview of neutron production rate from various targets at different electron beam energies is shown in Fig. 36.2 [166].

36.6 Measurement of Photoneutron Flux

As in the case of photoneutron production background gamma noise is inherently high therefore neutron flux is passively measured by Gold foil activation technique [178]. Gold foil is the preferred choice because it has large cross-section (98.65 barn) for thermal neutrons and insensitive to gamma. Upon getting irradiated with thermal neutrons, excited 198Au nuclei decays by emitting 411.8 keV gamma which is measured by high energy resolution gamma detector (BGO, HPGe or $LaBr_3$). Half life of excited ^{198}Au nuclei is 2.695 days.

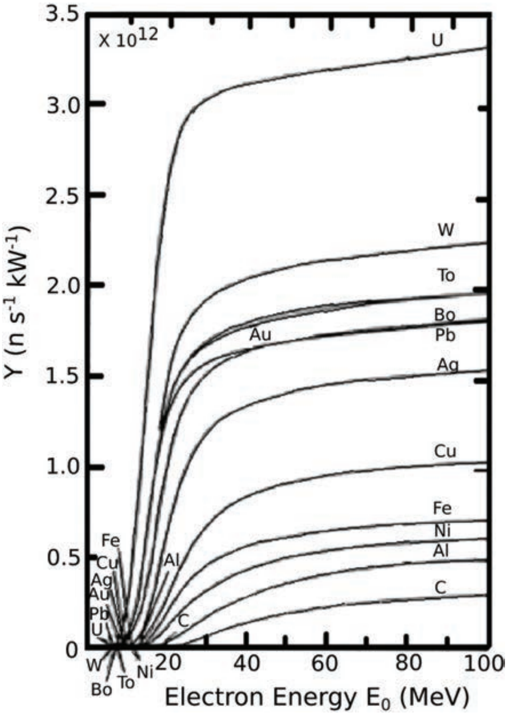

Figure 36.2: Neutron production rate (n/s for per kW of electron beam) for various materials at different electron beam energies [166].

36.7 Neutron Dosimetry

Though photoneutrons produced in LINAC's have broad distributed energy spectrum therefore radiological safety becomes an important concern. The 'Quality Factor' also known as 'Radiation Weighing Factor' (unit - rem/rad) is a value used in health physics to quantify how damaging the radiation is. Table 36.4 lists 'Quality Factors' designated for various neutron energies [178].

Table 36.4: 'Quality Factor' for various neutron energies [178].

Neutron Energy (MeV)	**Quality Factor**
2.5×10^{-8}–0.01	2
0.1	7.4
0.5	11
1	10.6
2	9.3
5	7.8
10	6.8
20	6

36.8 Summary

In the present date there is global thrust towards development of LINAC based neutron sources to cater application requirements in the field of medical, fundamental research, nuclear physics, material science, biotechnology etc. With the implementation of elaborated schemes in this chapter, contemporary electron LINAC's in the range of 5 MeV to 30 MeV can be suitably used for neutron production with large enough flux meeting variety of application requirements. The most important aspect of accelerator based neutron source which makes them versatile and preferred choice for wide range of applications is the scope of scalability of neutron flux. The neutron fluence increases with the subsequent increase of impinging electron beam energy. Recently we have successfully demonstrated the utilization of a 9 MeV RF Electron LINAC (at LTF, ECIL, Hyderabad) for neutron radiography application by implementing γ-n neutron production scheme. The pulsed coupled-cavity on-axis LINAC operates at a frequency of 2856 MHz with pulse width of $\sim$6 μs and 200 Hz repetition rate. The sub-assemblies of LINAC are horizontally aligned and the setup is shown in Fig. 36.3. The accelerated high energy electron beam produces maximum gamma dose rate

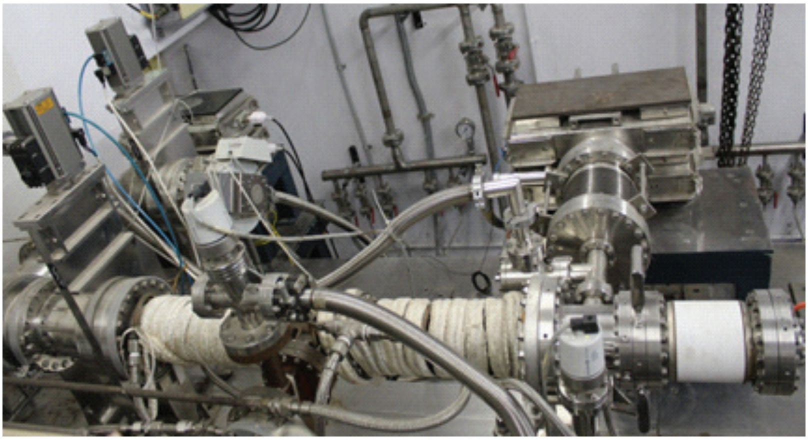

Figure 36.3: The 9 MeV, 1 kW coupled-cavity on-axis electron RF LINAC.

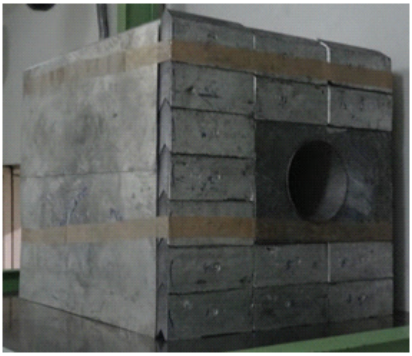

Figure 36.4: Photograph of photo-neutron target assembly setup used for neutron radiography.

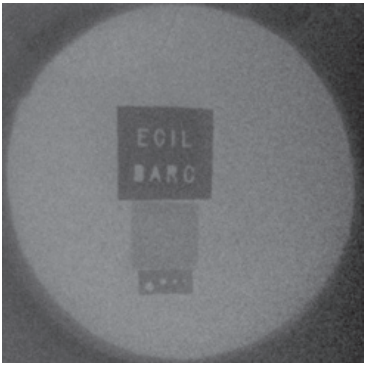

Figure 36.5: Obtained neutron radiograph of engraved cadmium stencil.

of ~24 Gy/min upon striking the water-cooled Tantalum target and thereafter gamma interacts with Beryllium producing photo-neutrons. For maximizing thermal neutron fluence, partly separated Beryllium cylinders of 63 mm diameter having lengths 44 mm and 84 mm have been used along with 60 mm thick high density polyethylene (HDPE) moderator in between. To minimize the gamma content at image plane, a lead collimator was centrally aligned in perpendicular direction to HDPE moderator that is in between two Beryllium targets. It has 500 mm length, 10 mm aperture and 150 mm image plane diameter. As shown in Fig. 36.4, the overall dimension of photo-neutron target assembly is 700 mm (L) × 855 mm (W) × 700 mm (H). Thermal neutron flux at image plane of collimator is $\sim 6 \times 10^3$ neutrons/cm^2/second/kW e-beam. For reducing gamma background, the entire photo-neutron target assembly was covered with 100 mm thick lead shielding and also the imaging with neutrons was done using Gated ICCD camera. By discretely gating the camera in time resolved manner, contribution of coincidently generated gamma with electron beam was selectively blocked and neutron radiograph of adequate resolution was obtained as shown in Fig. 36.5.